Double-Layered T-Shape Loaded Hairpin Resonator for High Performance Characteristic Dual Band BPF Design

zainab A. Mohammed (zainabaoda79@gmail.com)
University of Technology - Iraq
Raaed T. Hammed
University of Technology - Iraq

Research Article

Keywords: T-shape loaded hairpin resonator, double-layered filter, dual band BPF, multilayered TSLHR, compact dual band filter, multi-wireless network system

Posted Date: June 10th, 2022

DOI: https://doi.org/10.21203/rs.3.rs-1670251/v1

Double-Layered T-Shape Loaded Hairpin Resonator for High Performance Characteristic Dual Band BPF Design

[1]Zainab A. Mohammed and [2]Raaed T. Hammed

[1&2]Department of Electrical Engineering, University of Technology - Iraq, Baghdad, Iraq

E-mail: [1] zainabaoda79@gmail.com, [2]raaed.t.hammed@uotechnology.edu.iq

ORCID: [2](0000-0002-5372-9976)

Abstract: A simple high performance compact dual band bandpass filter is developed in this paper based on multilayered T-shape loaded hairpin resonator (T-SLHR). The filter circuit is constructed using two substrates. On the first ground plane substrate, two T-SLHRs are analyzed and electrically coupled through a space gap *S* to accomplish the desired dual passbands. To acquire the filtering response, an input/output grounded hairpin-stub is patterned on a second ungrounded-substrate and broadside coupled to the T-SLHRs. To validate the proposed concept, a dual-band BPF is realized for a multi-wireless network system working at 2.4 GHz and 3.5 GHz center frequencies. Indeed, the T-SLHR is analyzed based on odd-even theory to generate the specified frequencies. Furthermore, a block-diagram to explain the coupling mechanism of the expected filtering attitude is suggested. Moreover, the simulated filter is manufactured and its results from measurement and simulation are compared and discussed. The produced filter has quite small area less than 126 mm^2, high skirt roll-off selectivity and good isolation rejection band.

Keywords: T-shape loaded hairpin resonator, double-layered filter, dual band BPF, multilayered T-SLHR, compact dual band filter, multi-wireless network system.

1 Introduction

With the rise of new wireless technologies [1-5], compact and low cost high-performance microwave filters are highly recommended. However, dual-band bandpass filters with some or all these characteristics are developed using several design techniques and technologies [6-19]. Based on microstrip technology [6-11], dual narrow-passband filters are investigated using parallel stepped impedance open stubs in [6] and grounded stepped impedance resonator in [7]. Also, a traditional open/short microstrip-stubs are configured to realize dual passband filter with wide bandwidth performance [8]. In the same fashion, a dual-wide-passband BPF is realized in [9] with pending capability using paper substrate. Following the even-odd method, [10] proposed an open stub loaded coupled lines to develop a multi-band BPF with passband isolation enhancement. In Addition, a parallel coupled stepped-impedance resonator is adopted in [11] to produce a high-selectivity DB bandpass filter. Remote from microstrip technology, dual band BPF is introduced with quite large area using substrate integrated waveguide (SIW) technology [12, 13]. Moreover, hybrid technologies such as microstrip/DGS in [14, 15], microstrip/CPW in [16], and substrate integrated-DGS in [17] are suggested to design a multi-band passband filter. In spite of manufacturing difficulties, multilayer technology is very favored to develop miniaturized dual-band filters with good characteristic performance [18, 19].

In this work, a broadside coupled line of T-SLHR is proposed to design a miniature two-band bandpass filter. The T-SLHR is a multi-behavior resonator. Therefore, its resonance frequency is determined using even-odd analysis method. With the aid of the ADS software simulator the filter circuit is implemented and its characteristics are deeply studied. For practical purposes, an elliptical 2^{nd}-order DB-passband filter is fabricated and measured for a 2.4/3.5 GHz multifunctional wireless network. The measured response show good congruence with the simulated result.

2 T-SLHR Analysis And Frequency Characteristic

The transmission line configuration of the suggested T-shape loaded hairpin resonator is shown in Fig. 1a. The resonator is a superimposed shape consist of a traditional $\lambda_g/2$-haipin resonator loaded at the middle by a T-shaped open stub. However, the structure is a dual mode resonator. For the purposes of frequency analysis, the transmission line impedances and angle lengths of the T-SLHR, Fig. 1a, are characterized by ($Z_1, \theta_1, Z_2, \theta_2,\ Z_3, and\ \theta_3$). Following the odd-even method, the T-SLHR is analyzed and its frequency characteristic is determined.

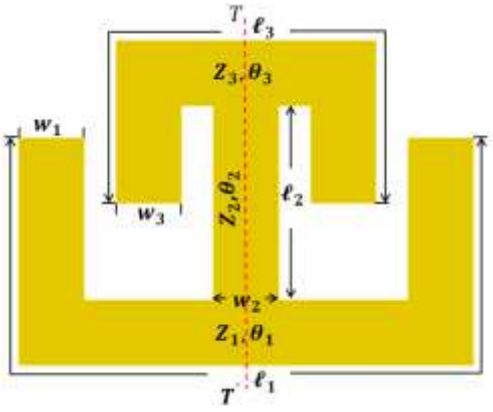

(a)

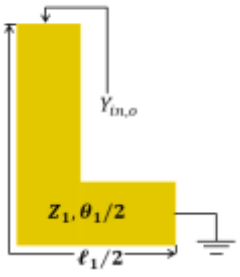

(b)

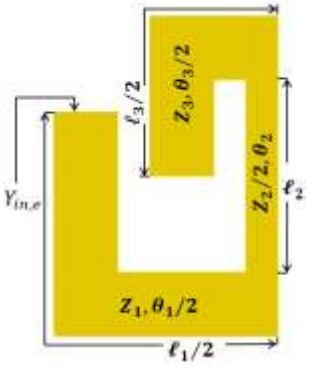

(c)

Fig.1. (a) Conductor pattern of the T-SLHR: (b) Odd-mode circuit model. (c) Even-mode circuit model.

As shown in Fig. 1, two equivalent circuits can be expected [20]. At odd-mode excitation, Fig. 1b, the input admittance is given as:

$$Y_{in,o} = \frac{Y_1}{jtan(\theta_1/2)} \tag{1}$$

where θ is the electrical length of the resonator ($\theta = \beta\ell$). Applying the resonance condition, $Y_{in,o} = 0$, the odd-resonance frequency is calculated:

$$f_o = \frac{c}{2\ell_1\sqrt{\varepsilon_{eff}}} \tag{2}$$

In the same fashion, the even-mode admittance, Fig. 1c, can be expressed as:

$$Y_{in,e} = -jY_1\frac{Y_a+Y_1\tan(\theta_1/2)}{Y_1-Y_a\tan(\theta_1/2)} \tag{3}$$

where $Y_a = Y_2/2\tan(\theta_2) + Y_3\tan(\theta_3/2)$. The resonance condition is, $Y_{in,e} = 0$. Hence the even-resonance frequency is given as:

$$f_e = \frac{c}{(\ell_1+2\ell_2+\ell_3)\sqrt{\varepsilon_{eff}}} \tag{4}$$

In this article, the dual mode T-SLHR, Fig. 1a, is designed with characteristic impedances of ($Z_1 = Z_2 = Z_3 = 39\,ohm$) to generate a desired 3.5 GHz-odd and 2.4 GHz-even resonance frequencies. Adopting the above equations, the T-SLHR physical dimensions are computed based on Rogers Ceramic RO4360 substrate has a dielectric constant of $\varepsilon_{r1} = 6.15$ and a thickness of $h_1 = 0.508\,mm$. The calculated dimensions are summarized in Fig.2. Next, the proposed resonator, Fig. 1a, is simulated using advanced design system (ADS) software program [21], and its characteristic frequency is reported in Fig. 2. Reading the imaginary part of the T-SLHR input admittance, it is clear that the resonator has two original frequencies one at even-characteristic frequency ($f_e = 2.4\,GHz$) and the second at odd-characteristic frequency ($f_o = 3.5\,GHz$).

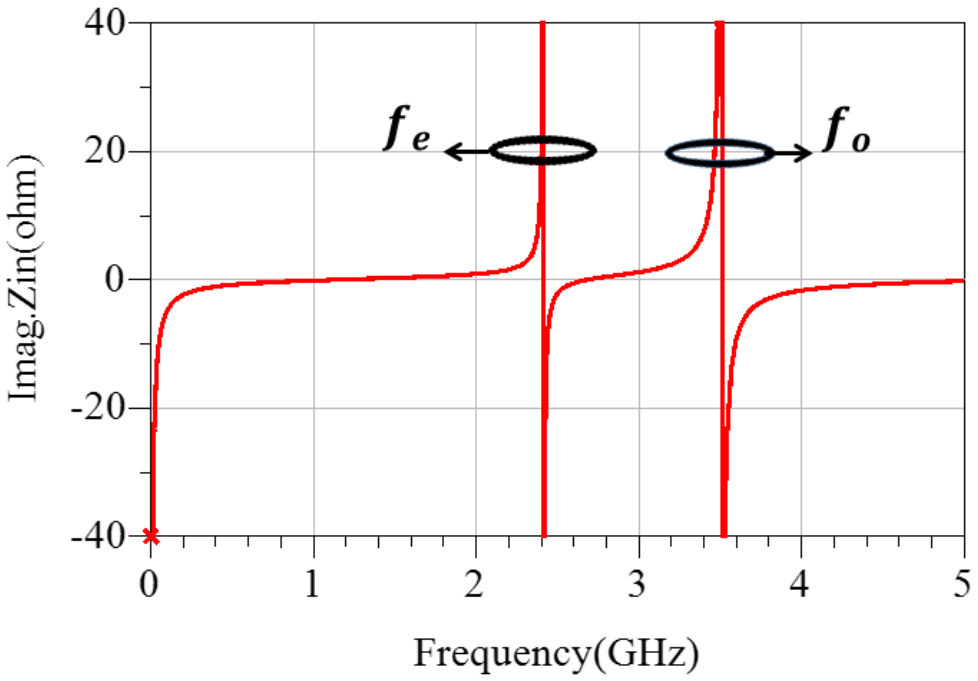

Fig. 2. Input admittance characteristic frequency of the suggested T-SLHR $\ell_1 = 17.6mm$, $\ell_2 = 6.75mm$, $\ell_3 = 13mm$, $w_1 = 1mm$, $w_2 = 1mm$, $w_3 = 1mm$.

3 Dual Band BPF Design Methodology

Due to its symmetry, the suggested T-SLHR in section 2 is analyzed based on even-odd analysis method and its characteristic frequencies (f_e&f_o) are calculated at 2.4 GHz and 3.5 GHz respectively. These frequencies are the desired center frequencies of the proposed dual passbands. The filter conductor circuit is patterned in three-layer configuration using two substrates, Fig. 3a. On the bottom ground plane substrate, two identical T-SLHRs are designed and capacitively-coupled through a coupling space S to realize and control the specified passbands. To achieve the filtering attitude, an input/output grounded hairpin-stub is formed on a top ungrounded-substrate and vertically-coupled to the bottom circuit, Fig. 3a. It is good to notice that the input/output coupling strength can be easily controlled through the thickness of the top substrate h_2 .

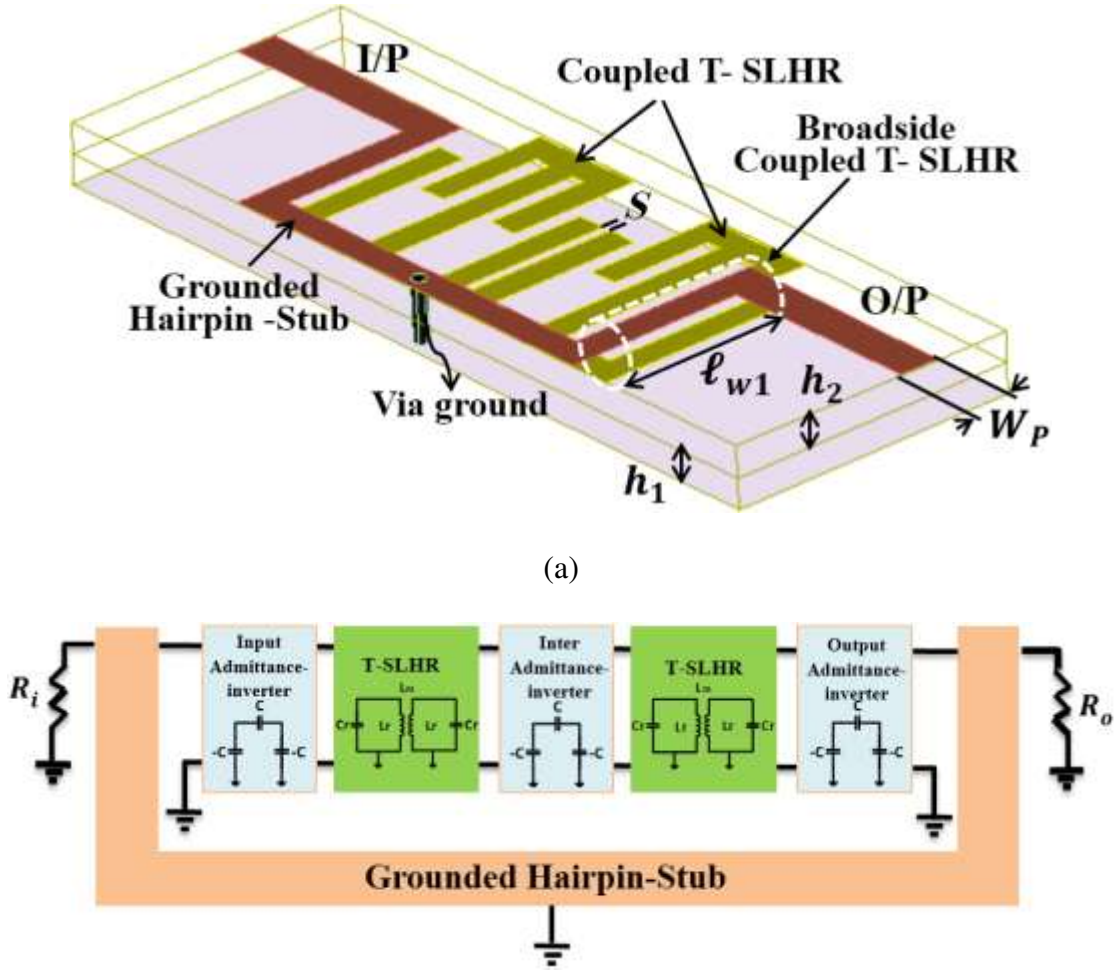

Fig.3 The developed dual-band BPF using multilayered T-SLHR: (a) A three-dimension configuration. (b) Coupling mechanism block diagram.

To support the above concept and describe the expected filtering attitude, a block-diagram for its behavior is suggested in Fig. 3b. In principles [22, 23], a dual mode resonator can be consider as a two LC-coupled resonator. Also, the coupling mechanism in this work is an electrical-coupling which is equivalent to an admittance-coupling. However, the expected frequency response is divided to three basic regions: the rejection-band regions ($f < f_e, f_e < f < f_o, and\ f > f_o$), the even-passband region ($at\ f_e$), and the odd-passband region ($at\ f_o$). At the rejection-band regions, the signal will pass through the

input/output grounded hairpin-stub which give the advantage to generate a favourite transmission zeros around the desired passbands. In case the signal is closed or at the desired even/odd-passband regions, it will pass via the admittance-coupling capacitors and the resonant T-SLHRs, Fig. 3b. Herein, two transmission poles at each passband can be obtained and hence 2nd-order elliptical dual-band BPF.

To investigate the filtering response performance, two T-SLHRs with the above mentioned physical dimensions, Fig. 1a, are etched and coupled via distance coupling S using a ground plane Rogers Ceramic RO4360 substrate with relative permittivity of $\varepsilon_{r1} = 6.15$ and thickness of $h_1 = 0.508\,mm$. Using a second ungrounded Rogers Ceramic RO4360 substrate with relative permittivity $\varepsilon_{r2} = 6.15$ and thickness h_2 , an input/output grounded hairpin-stub of $\ell_{total} = 27.3mm\ and\ w_1 = 1mm$ is constructed and directly connected to a 50-ohm feeding ports of $w_p = 1.37mm$, Fig. 3a. Next, the two circuits are broadside coupled through $\ell_{w1} = 6.3mm$ and simulated. Using a loss coupling distance of $h_2 = 1.5mm$, the passband performance is studied with variable gap coupling $S = (0.6 - 0.3)mm$ as shown in Fig. 4. Obviously, the two passbands can be controlled in which the narrower gap lead to a wider bandwidth. Also, it can be notice that the coupling strength at the odd-passband is stronger than the coupling strength at the even-bassband. In the same fashion, the filtering response is also investigated, Fig. 5, with fixed $S = 0.3mm$ and various values of $h_2 = (2 - 0.5)mm$. Reading the results in Fig. 5, the input/output coupling strength can be controlled in which the closer h_2 the enhanced filtering response. However, still the coupling strength at the even-basspand is not enough to generate a good filtering attitude. To increase the even-coupling strength, a short open-stub with physical dimensions of $\ell_4 = 7mm\ and\ w_4 = 1mm$ is performed at the top of the T-shaped stubs, Fig. 6a. With aid of the momentum ADS simulator, the optimized filter is accomplished at $S = 0.3mm\ and\ h_2 = 0.5\,mm$, Fig. 6b. Clearly, this figure show that the proposed filter is a second-order filter offering bandwidths of 0.11/0.3 GHz with $|S_{21}|/|S_{11}|$ losses of 0.66/25.6 dB at even-passband and 0.58/15.7 dB at odd-

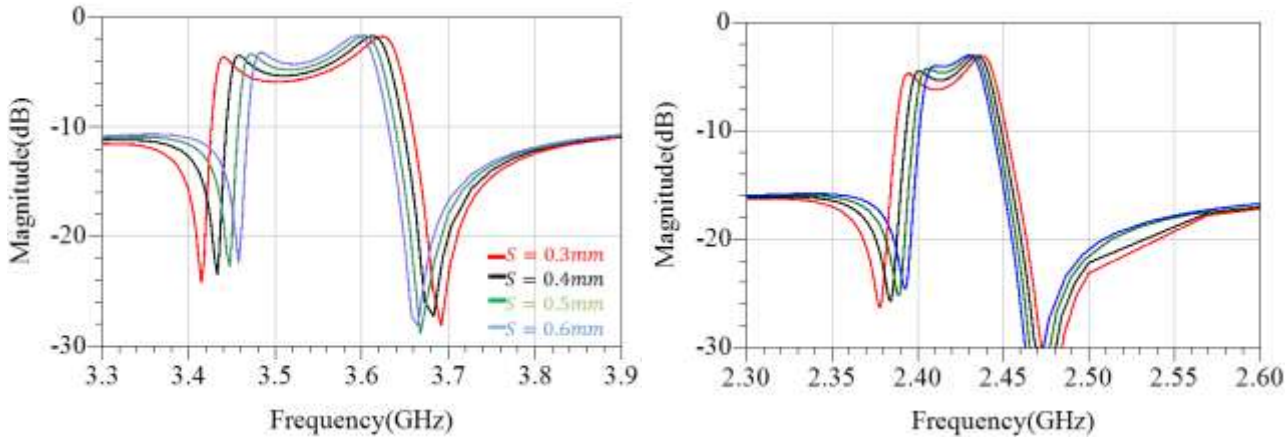

(a) (b)

Fig. 4. Simulated $|S_{21}|$ of the broadside coupled T-SLHR dual band BPF, Fig.3: (a) odd-passband, and (b) even-passband.

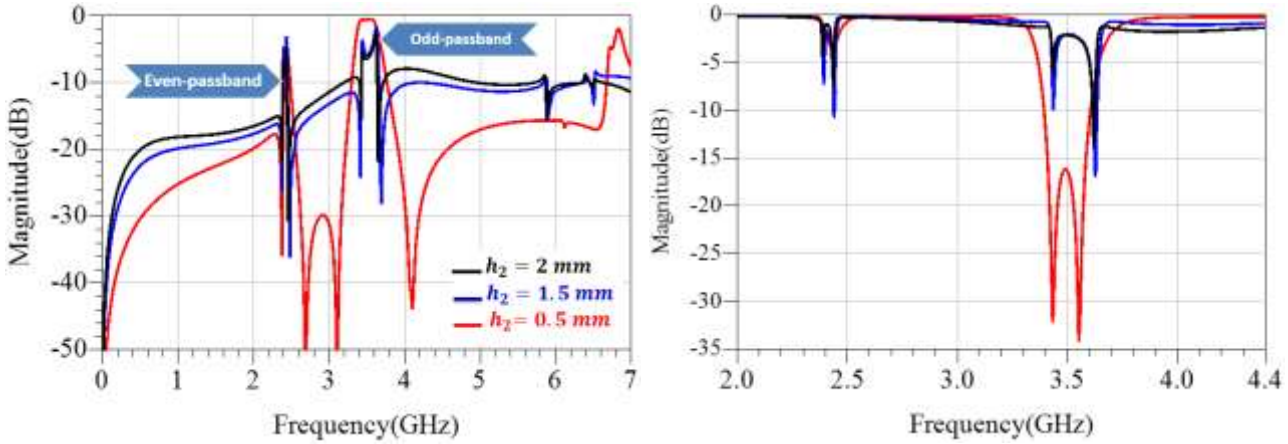

(a) (b)

Fig. 5. Simulated S-parameters of the broadside coupled T-SLHR dual band BPF, Fig.3: (a) Insertion loss, and (b) Return Loss.

passband. In addition, the response show good isolation, high-skirt selectivity, and wide stopband performance about 3 GHz at -15 dB. All these performance are achieved with a quite small circuit area of 125.1 mm^2.

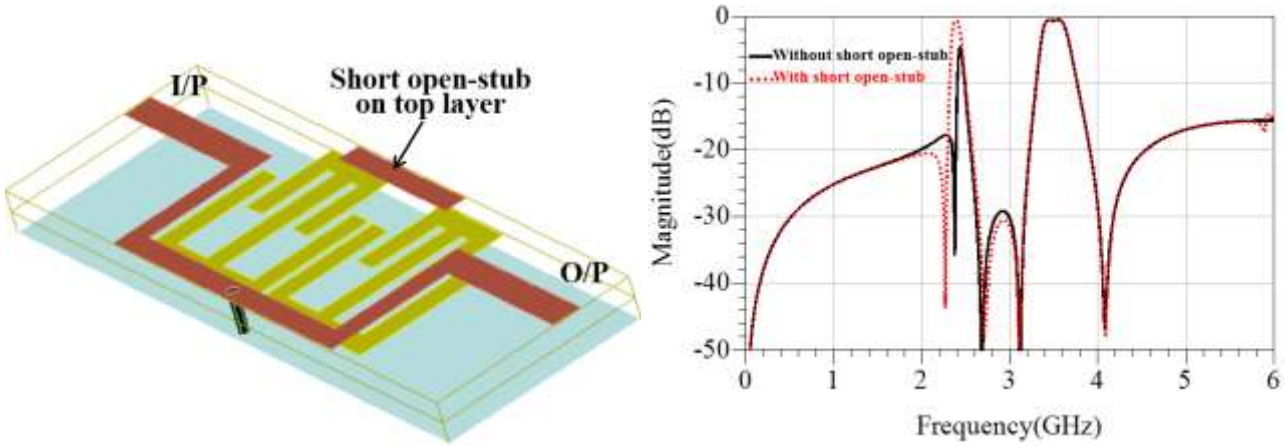

(a) (b)

Fig. 6 Optimized dual band BPF with short open-stub: (a) The three-dimension geometry. (b) The filtering response from insertion loss

For the purpose of practical verification, the optimized dual band BPF is fabricated, Fig. 7a, and its S-parameter response are carried out using Anritsu MS4642A Vector Network Analyser. The insertion and return losses from measurement and simulation are compared and sketched in Fig. 7c. Reading the figure carefully, one can realize there is a good matching between the measured and simulated results. Unfortunately, the responses from measurement are altered with insertion loss, Fig. 7b. This is due to the fabrication process difficulties such as the vertical-aliment process. Also, utilizing a crystal-bond mounting adhesives to gather the dual band filter circuits will increase the thickness h_2 and decrease the required input/output coupling strength. Moreover, the relative permittivity of the crystal-bond will affect the electromagnetic field distribution in the bottom circuit and may change the response. Regardless, Table 1 shows the potential of the simulated dual band BPF when compared to the recently reported dual band BPFs.

(a) (b)

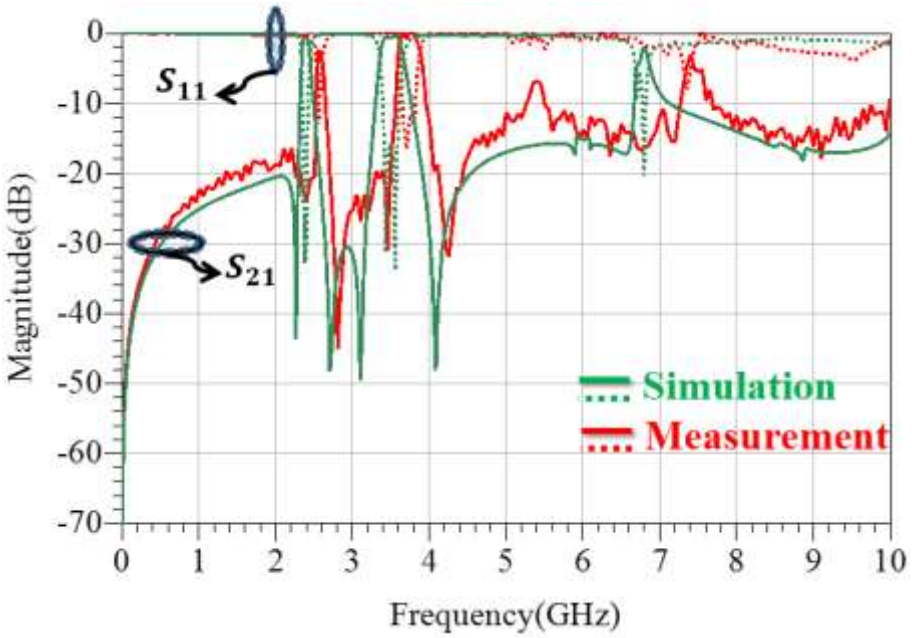

(c)

Fig. 7 Manufactured broadside coupled T-SLHR dual band BPF: (a) Before broadside aliment. (b) After broadside aliment. (c) Simulated and measured filtering response.

Table I. Comparison among the presented filter and previously reported works

Ref.	$f_o\,(GHz)$	**Selectivity & No. of Tzs**	**Controlled B.W**	**Rejection band Perf. (GHz/dB)**	**Isolation**	**Circuit size** $(\lambda_g \times \lambda_g)$
[6]	5.7/ 6.5	Poor/1	no	12/20	Poor	0.22×0.11
[8]	2.4/5.2	poor/4	yes	1.6/10	good	0.28×0.20
[13]	2.25/3.29	Poor/1	no	0.7/20	poor	0.24×0.24
[11]	2.33/4.36	Good/6	no	1.2/20	good	0.28×0.23
[19]	2.38/4.98	Good/4	no	3.25/15	good	0.18×0.20
This work	**2.4/3.5**	**Good/6**	**yes**	**2.8/15**	**good**	$\mathbf{0.24 \times 0.14}$

4 Conclusion

Based on multilayered T-shape loaded hairpin resonator, a simple design method to develop high performance compact dual band BPF was demonstrated in this letter. The T-SLHR frequency characteristics were obtained using even-odd analysis. Next, the desired passbands were realized and controlled when two T-SLHRs patterned and coupled on ground plane substrate. For filtering response verification, an input/output grounded hairpin-stub was implemented on ungrounded-substrate and vertically integrated to the coupled T-SLHR substrate. The proposed concept was supported by a coupling mechanism block diagram. At the end, a 2^{nd} –order dual band BPS filter was simulated, fabricated, and measured to serve a multi-wireless network working at 2.4/3.5 GHz. The filter s-parameter results from simulation and measurement were compared and discussed. However, they were found in good agreement. The filter performance was distinguished with circuit area less than $126\ mm^2$.

Ethical Approval

"Not applicable for that specific section"

Consent to Participate

"Not applicable for that specific section"

Consent to publish

"Not applicable for that specific section"

Authors Contributions

"All authors contributed to the study conception and design. Material preparation, data collection and analysis were performed by [**[1]Zainab A. Mohammed**], [**[2]Raaed T. Hammed**]. The first draft of the manuscript was written by [**[2]Raaed T. Hammed**] and all authors commented on previous versions of the manuscript. All authors read and approved the final manuscript"

Funding

“The authors declare that no funds, grants, or other support were received during the preparation of this manuscript”

Competing Interest

“The authors have no relevant financial or non-financial interest to disclose”

Availability of Data and materials

“The datasets generated during and/or analysed during the current study are not publicly available due to [this work is part of my MSc study which still I am working on] but are available from the corresponding author on reasonable request”

References

1. Hammed, R. T. (2015). Compact Marchand balun circuit for UWB application. *AEU-International Journal of Electronics and Communications*, *69*(5), 851-855.

2. Karimi, G., & Babakan, A. (2015). Novel Compact Microstrip Stepped-Impedance Resonator Using Computational Approach and Application to Dual-Band Bandpass Filters. *Wireless Personal Communications*, *82*(4), 2311-2322.

3. Hammed, R. T. (2015). Miniaturized high-order ultra-wideband bandpass filters with multiple band rejection notches. *Electromagnetics*, *35*(8), 538-549.

4. Hammed, R. T. (2015). Miniaturized high-order ultra-wideband bandpass filters with multiple band rejection notches. *Electromagnetics*, *35*(8), 538-549.

5. Shirkhar, M. M., & Roshani, S. (2022). Design and Implementation of a Bandpass–Bandpass Diplexer Using Coupled Structures. *Wireless Personal Communications*, *122*(3), 2463-2477.

6. Najafi, M., & Hazeri, A. R. (2021). Microstrip dual-narrowband bandpass filter with independent passbands. *Wireless Personal Communications*, *119*(4), 3503-3516.

7. Hammed, R. T., & Abbas, S. M. (2021). A Small Dual Narrowband BPF with Ultra-Rejection Band Using Grounded Stepped-Impedance Resonator. *IETE Journal of Research*, 1-6.

8. Liang, G. Z., & Chen, F. C. (2020). A compact dual-wideband bandpass filter based on open-/short-circuited stubs. *IEEE Access*, *8*, 20488-20492.

9. Kumar, K. V. P., Velidi, V. K., Althuwayb, A. A., & Rao, T. R. (2021). Microstrip Dual-Band Bandpass Filter With Wide Bandwidth Using Paper Substrate. *IEEE Microwave and Wireless Components Letters*, *31*(7), 833-836.

10. Kishore, S., Arora, A., V. Phani Kumar, K., Velidi, V. K., Nayak, C., Rao, T. R., & Rajkumar, R. (2021). Compact dual-band bandpass filter with high-passband isolation using coupled lines and open stub. *Microwave and Optical Technology Letters*, *63*(11), 2710-2714.

11. Li, D., Wang, J. A., Liu, Y., Chen, Z., & Yang, L. (2021). Selectivity-enhancement technique for parallel-coupled SIR based dual-band bandpass filter. *Microwave and optical technology letters*, *63*(3), 787-792.

12. Zhang, H., Kang, W., & Wu, W. (2018). Miniaturized dual-band SIW filters using E-shaped slotlines with controllable center frequencies. *IEEE Microwave and Wireless Components Letters*, *28*(4), 311-313.

13. Fei, H., Wang, Y., Zhang, Q., Zhou, L., Chen, W., & Chen, C. (2021). Miniaturized single-/dual-band bandpass filters based on grounded square patch resonator with controllable passbands. *Microwave and Optical Technology Letters*, *63*(6), 1688-1692.

14. Moitra, S., & Dey, R. (2020). Design of dual band and Tri-band Bandpass Filter (BPF) with Improved inter-band isolation using DGS integrated coupled microstrip lines structures. *Wireless Personal Communications*, *110*(4), 2019-2030.

15. Challal, M., Hocine, K., & Mermoul, A. (2019). A novel design of compact dual-band bandpass filter for wireless communication systems. *Wireless Personal Communications*, *109*(3), 1713-1726.

16. Xu, S., Meng, F., Ma, K., & Yeo, K. S. (2019, June). Dual-band Bandpass Filter Design with Novel Double-layer Mixed Coupled SIR/CPW-SIR Resonators. In *2019 IEEE Mtt-S International Microwave Symposium (Ims)* (pp. 714-717). IEEE.

17. Tang, D., Han, C., Deng, Z., Qian, H. J., & Luo, X. (2020). Substrate-integrated defected ground structure for single-and dual-band bandpass filters with wide stopband and low radiation loss. *IEEE Transactions on Microwave Theory and Techniques*, *69*(1), 659-670.

18. Hammed, R. T. (2015). Miniaturized dual-band bandpass filter using E-shape microstrip structure. *AEU-International Journal of Electronics and Communications*, *69*(11), 1667-1671.

19. Chang, H., Sheng, W., Cui, J., & Lu, J. (2020). Multilayer dual-band bandpass filter with multiple transmission zeros using discriminating coupling. *IEEE Microwave and Wireless Components Letters*, *30*(7), 645-648.

20. M. Makimoto and S. Yamashita, *Microwave resonators and filters for wireless communication*, 2001, Berlin:Springer.

21. Advanced Design System (ADS) 2017a. Palo Alto.CA, Agilent Technol., 2017.

22. J. S. Hong and M. J. Lancaster, *Microstrip filters for RF/Microwave applications*. 2001, New York:Wiley.

23. Hammed, R. T., & Mirshekar-Syahkal, D. (2011, October). A lumped element equivalent circuit of E-shape microstrip structure for UWB filter design. In *2011 41st European Microwave Conference* (pp. 651-654). IEEE.